

Sulfurization and Antibacterial Properties of ZnS/ZnO Coreshell Structures on Glass Fibers

Jiun-Jr Wang¹, Cheng Yuan Li², Wei-Chih Weng², Jo Lun Chiu², Yan Yu Chen², Chen Haw Su², Yu Sheng Tsai² and Hsiang Chen^{2,*}

¹School of Medicine, Fu Jen Catholic University, New Taipei City, Taiwan, ROC

²Applied Materials and Optoelectronic Engineering, National Chi Nan University, Taiwan, ROC

Received: January 08, 2018, Accepted: December 10, 2018, Available online: January 18, 2019

Abstract: In this research, we synthesized ZnO/ZnS shell nanostructures on the surface of glass fiber. With multiple analyses of field emission scanning electron microscope (FESEM), energy dispersive spectrometer (EDS), Photoluminescence (PL) and X-ray diffraction (XRD), we examined the material properties of ZnO/ZnS nanostructures grown at various time. In addition, we assessed the antibacterial property of ZnS/ZnO core-shell structures on glass fibers by OD 600 technique.

Keywords:

1. INTRODUCTION

Zinc oxide (ZnO) is a non-toxic, multifunctional material that exhibits photoelectric [1,2,3,4], photocatalytic [5,6,7], photoelectric and antibacterial capacity [8,9,10,11]. Since ZnO has hexagonal non-central symmetric structure, it is also a piezoelectric material [1,2,3,4]. Besides, ZnO can absorb inorganic UVA and UVB, and it has been grown on glass fiber and other composite materials as a radiation absorbent against UV damages [12,13,14]. When ZnO grows on a glass fiber, it also exhibits antibacterial and anti-corrosion capacity [15]. Glass fiber has the characteristics of high temperature, non-burning, good shape stability, good electrical insulation, chemical resistance to corrosion. Glass fiber can be made of glass fiber filters [16].

ZnS is a semiconductor material. When ZnS grows with ZnO as a ZnO/ZnS composite material, it exhibits several superior properties including anti-bacterial capacity [17,18,19,20]. ZnO/ZnS shell structure has been used in sensor synthesis, and until now, it has not been grown on glass fiber. In this study, we employed the hydrothermal method to manufacture ZnO/ZnS shell nanostructures on the surface of glass fibers. We verified ZnO/ZnS shell structure using X-ray diffraction (XRD) and high resolution X-ray photoelectron spectrometer (XPS), Photoluminescence (PL) and examined the nanostructure morphology via magnification field emission scanning electron microscope (FESEM), chemical property by Energy Dispersive Spectrometer (EDS), and antimicrobial test via OD 600 test.

2. EXPERIMENT

A large piece of glass fiber was cut into smaller pieces of size 2 cm² cm. Glass fibers were washed in a ultrasonic shock washing machine for 10 min, with a solution containing ethanol, acetone and isopropyl alcohol. Samples were then heated in an oven to remove solvents. The spinnerette was placed on a spin coater, and spin-coated at 500 rpm for 5 s, followed by 3000 rpm for 25 s, and then heated on a hot plate at 130 °C. Glass fibers, placed on a clean silicon substrate, were dried on a hot plate, before spin-coating, then repeated the process four more times. ZnO seed layer was then deposited on the surface of glass fiber, which in turn was placed on a clean silicon substrate and fixed with a checkered needle on a slide to keep the glass fiber from falling during the process of hydrothermal and vulcanization. To grow ZnO nanostructure, glass fibers, placed in a serum bottle containing 100 ml of 0.05 M zinc nitrate hexahydrate and 0.07 M hexamethylenetetramine, were incubated at 80 °C for 1 hour, and then dried.

Glass fibers, placed in a solution of 100 ml containing 0.1 M sodium sulfide nine water compound, were subjected to 5, 10, 15 or 20 min incubation at 70 °C, and then processed for S²⁻/O²⁻ exchange.

In this study, FESEM analysis was used to examine the growth of ZnO structure and ZnO/ZnS shell nanostructures. EDX, XPS and XRD analysis were used to assess the sample compositions and chemical bonding and crystal structure, respectively. OD 600 test was adopted for antimicrobial test, and we also conducted corrosion resistance test.

*To whom correspondence should be addressed: Email: hchen@nccu.edu.tw
Phone: 886-49-2910960

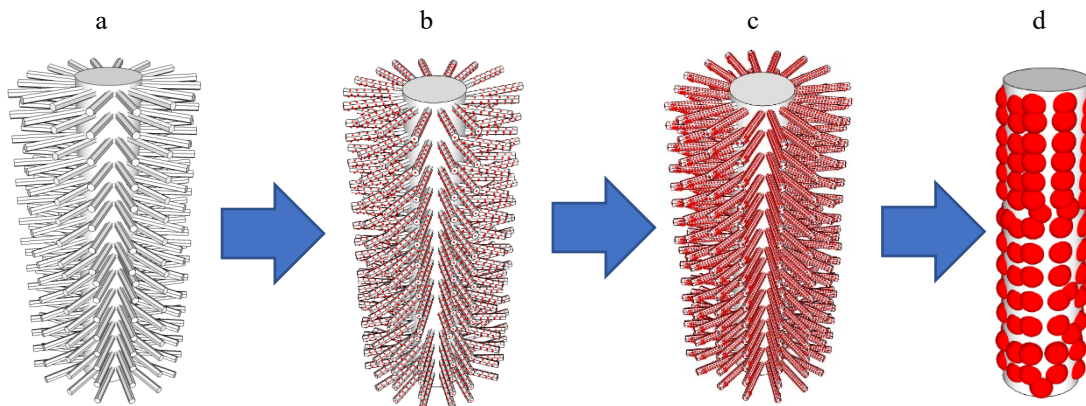


Figure 1. 3D illustration of the growth process of ZnO to ZnO/ZnS

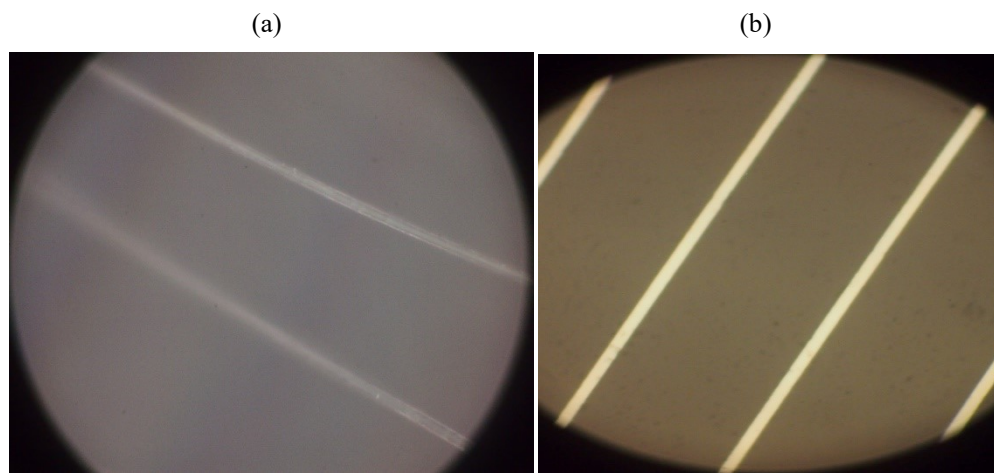


Figure 2. (a) The OM chart of the length of ZnO nanocolumn of the glass fiber. (b). The scale between mesh is 100 μm .

3. RESULTS AND DISCUSSION

Fig. 1 is a schematic view of ZnO nanorods and ZnS shell grown on glass fiber. Fig. 1-a shows the growth of ZnO nanorods on glass fibers only. Fig. 1-b to d show the growth of ZnS shells on ZnO nanorods. As the time of ZnS grew longer, the ZnS shell grew denser but eventually disintegrate.

Fig. 3 shows the growth of ZnO nanostructures on glass fibers analyzed by FESEM. The structure of ZnO was cylindrical and the surface of ZnO was smooth prior to the growth of ZnS (Fig 3a). As demonstrated from Fig 3(b) through (e), ZnS crystals grew with respect to time until the cylindrical shape of ZnO was completely covered at 20 min, and the roughness of the ZnO's surface strongly correlated with the level of growth of ZnS. EDS analysis revealed that the ratio of sulfur in the glass fiber increased with respect to time but started to decrease after 20 min, suggesting disintegration of some ZnS.

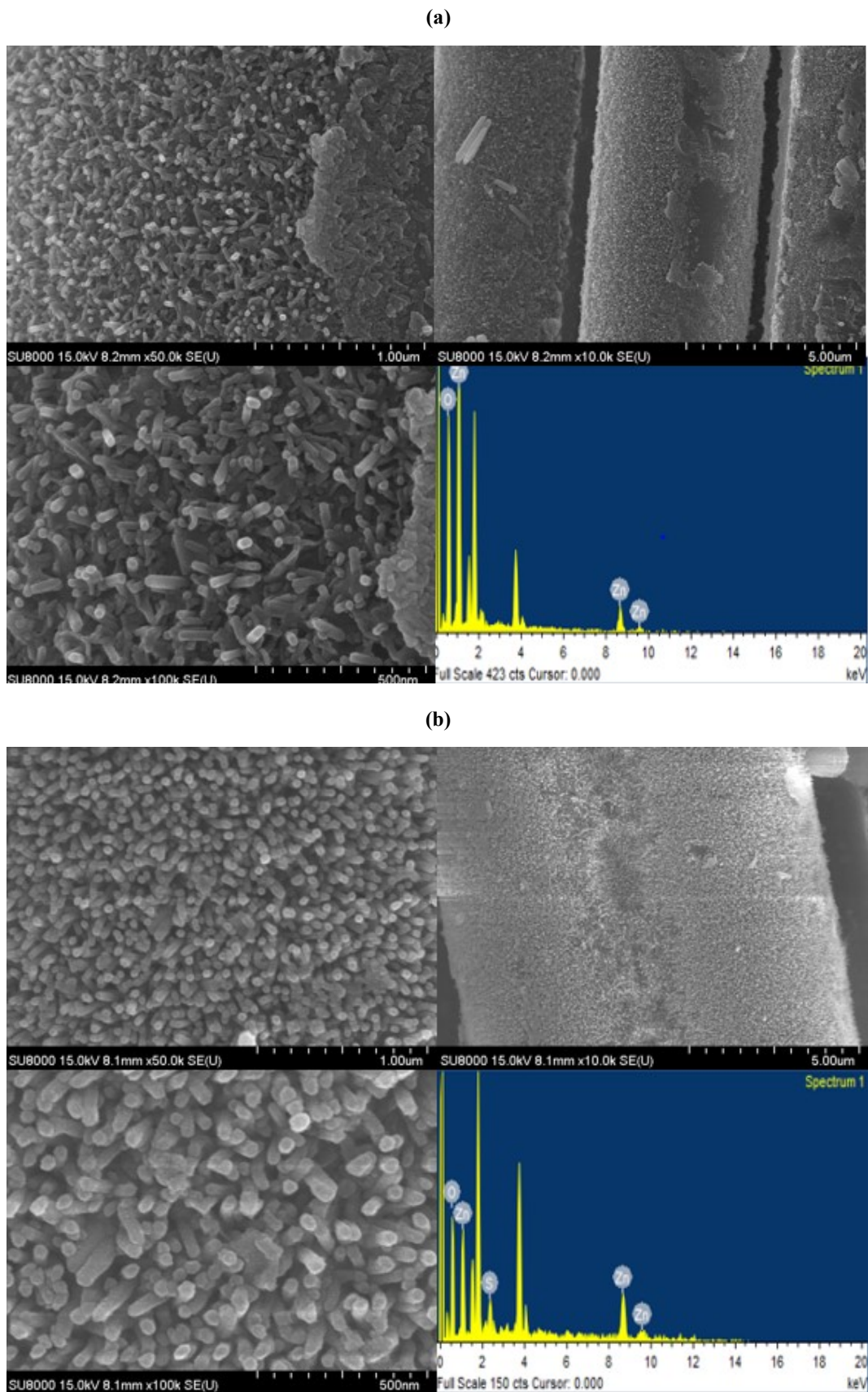
XRD analysis of ZnO fiber revealed a peak of ZnS at (111) and 3 peak of ZnO at (100), (002) and (101), respectively (Fig. 4). The highest peak of ZnO at (002) indicated that ZnO was both columnar and tended to grow c-axis. In addition, the high peak of ZnS at (111) represented the surface of ZnO covered by ZnS shell structure. The thickness of ZnS shell structure correlated with the crystal

growing time. However, EDX analysis revealed that the ratio of sulfur in glass fiber started to decrease beyond 20 min, suggesting disintegration of ZnS after 20 min. Since the ZnS shell is still on the substrate following disintegration, the result of XRD analysis still shows the longer ZnS growing time, the larger the peak of ZnS.

XPS analysis of glass fiber revealed a clear peak for sulfur, indicating complete coverage of ZnO by ZnS shell nanostructures (Fig. 5). The size of the peak of sulfur of ZnS at 10 min was higher than that of ZnS at 20 min. EDX showed a reduction in sulfur in fiber glass when the growth of ZnO was beyond 20 min that indicated disintegration of ZnS after 20 min.

OD 600 antibacterial test was conducted on ZnS shell synthesized on ZnO glass fiber at 5, 10, 15 and 20 min (Fig. 6). Results showed that glass fiber with either ZnO or ZnO/ZnS shell structures synthesized on the surface exhibited antibacterial capacity, and its effectiveness was positively associated with the amount of ZnS. The antibacterial effectiveness reached its maximum at 15 min and declined afterwards, and that was likely attributed to the disintegration of ZnS.

It can be seen from the photoluminescence (PL) spectrum that ZnO has two absorption regions, 380 nm and 550 nm. The peak of



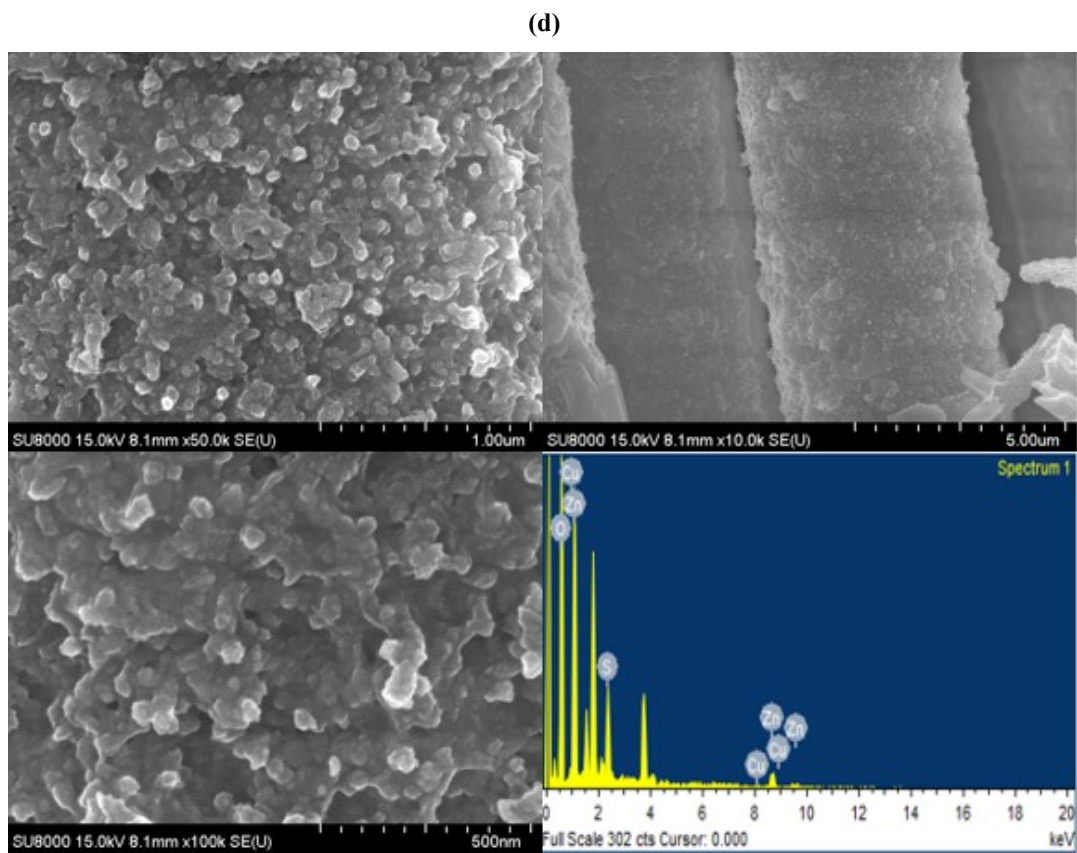
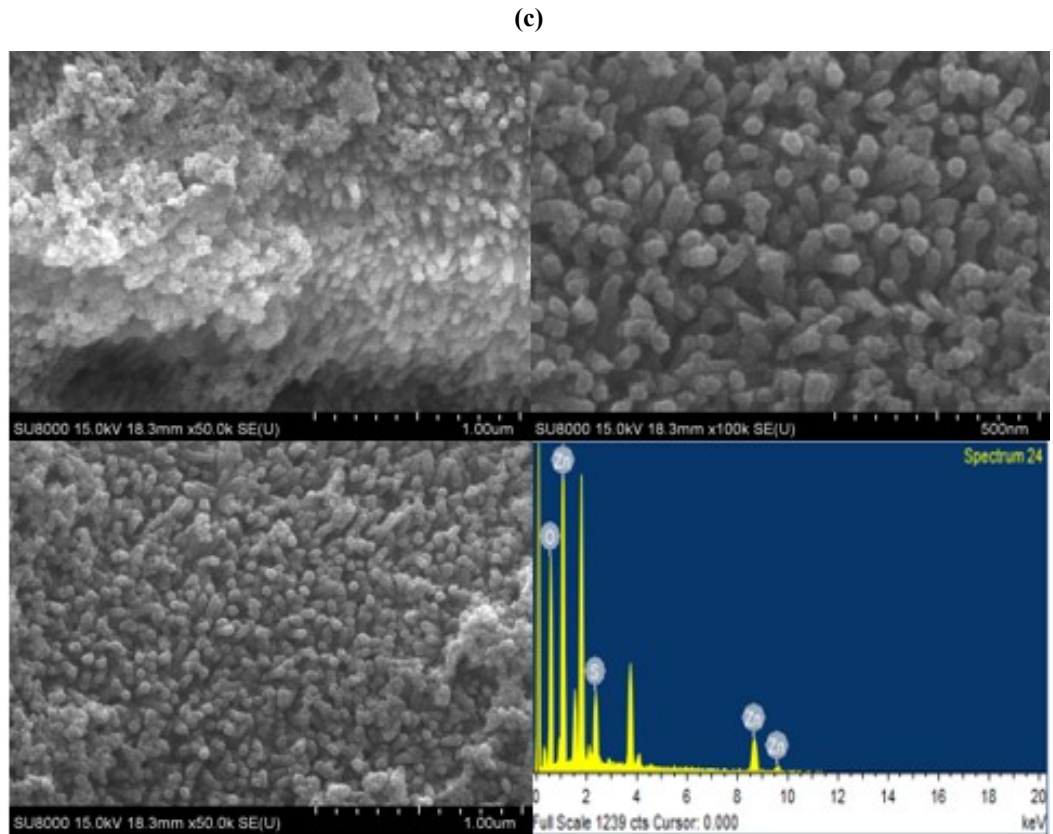


Figure 3-2. FESEM images and EDS analysis of ZnS/ZnO core-shell nanostructures grown at 10 (c), 15 (d).

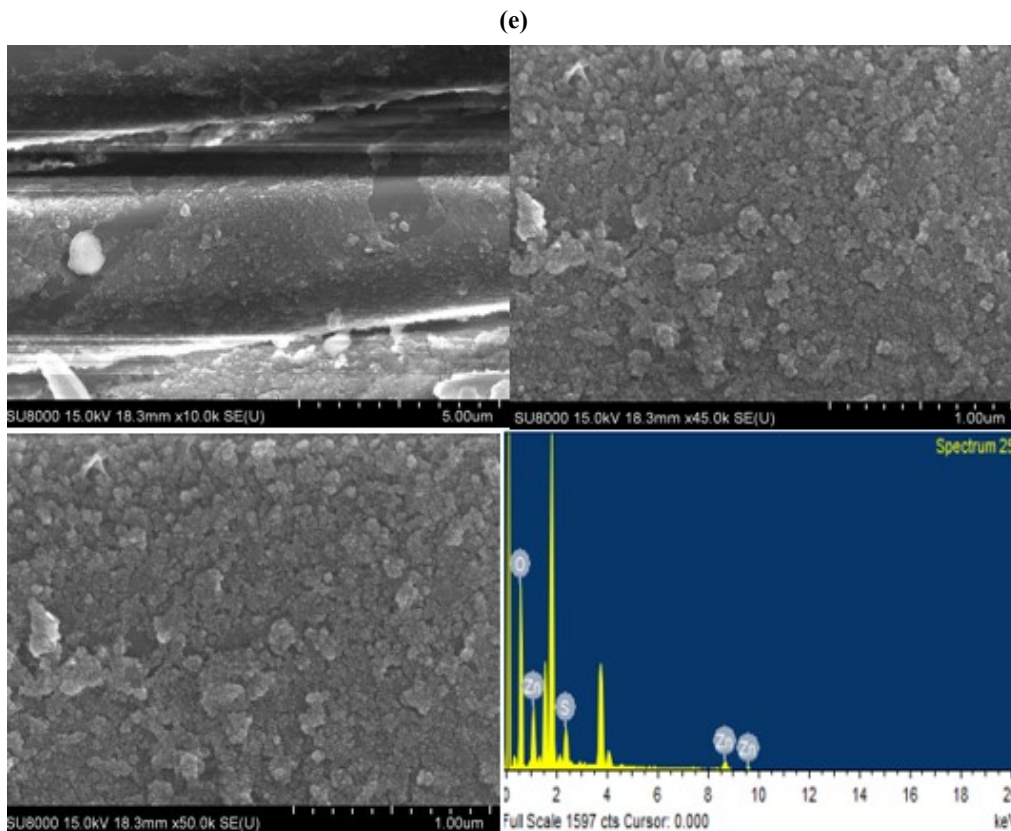


Figure 3-3. FESEM images and EDS analysis of ZnS/ZnO core-shell nanostructures grown at 20 min (e).

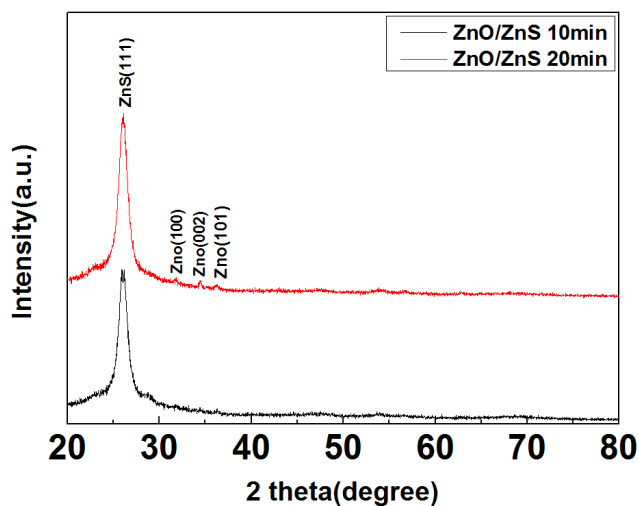


Figure 4. XRD patterns of the ZnO/ZnS on the glass fiber at 10 (black) and 20 min (red).

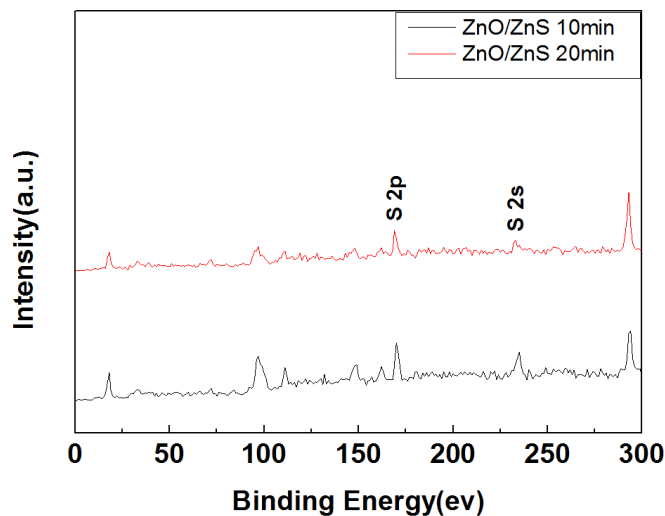


Figure 5. 0-300eV XPS measurement of the ZnO/ZnS on the glass fiber 10 mins and 20 mins.

ZnO is at 380 nm. When the ZnS shell increases, ZnO NRs are covered by ZnS, so that the peak value of ZnO decreased (Fig.7). The peak at 550 nm is due to crystal defects, mainly oxygen vacancies, since the oxygen of ZnO is replaced by sulfur and the emission intensity is decreased.

4. CONCLUSION

We employed the hydrothermal coating technique to synthesize ZnS nanostructure on the surface of ZnO, and that was verified by FESEM analysis. The growth of ZnO shell structure, analyzed by

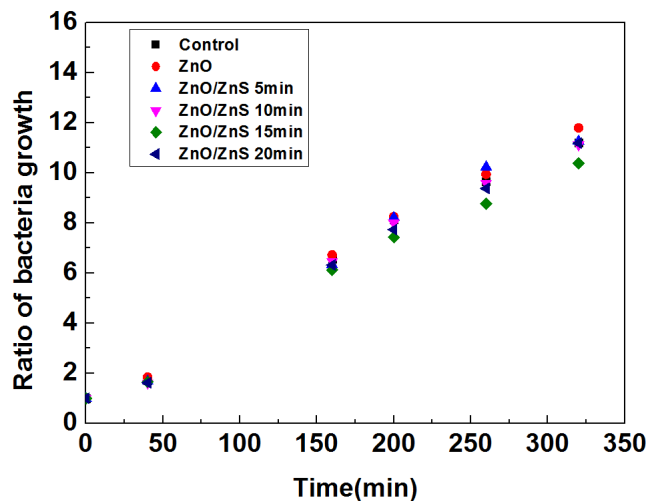


Figure 6. OD 600 antibacterial tests on ZnO alone and ZnO/ZnS on the glass fiber at 5, 10, 15 and 20 min.

EDX, was proportional with respect to time until 20 min, then decreased afterwards, and that was attributed to the disintegration of ZnS after 20 min. Besides, XPS analysis showed that the peak of ZnS at 10 min was higher than that of ZnS at 20 min, support disintegration of ZnS at 20 min. OD 600 tests revealed that the antibacterial effectiveness augmented along with the growth of ZnS crystals, and that decreased after 20 min, consistent with the disintegration of ZnS after 20 min. From PL analysis, it was found that the ZnO nanorods were successfully covered by the ZnS shell structure and covered more with time. However, XRD analysis showed that although the ZnS shell structure disintegrated at 20 minutes, these collapsing shells will still cover the substrate, making the peak of ZnS still strong, as can be observed from the PL analysis. We successfully synthesized ZnS/ZnO nanostructures that exhibited good antibacterial capacity and that can be applied to biosensors synthesis in the future.

REFERENCE

- [1] D. Crisler, J. Cupal and A. Moore, Proceedings of the IEEE, 56, 225 (1968).
- [2] Q. Yang, X. Guo, W. Wang, Y. Zhang, S. Xu, D. H. Lien and Z. L. Wang, Acs Nano, 4, 6285 (2010).
- [3] S. Dai and H. S. Park, Journal of the Mechanics and Physics of Solids, 61, 385 (2013).
- [4] J. Cembrero, A. Elmanouni, B. Hartiti, M. Mollar and B. Mar, Thin Solid Films, 451, 198 (2004).
- [5] V. Rogé, C. Guignard, G. Lamblin, F. Laporte, I. Fechete, F. Garin, A. Dina and D. Lenoble, Catalysis Today, (2017).
- [6] E. S. Elmolla and M. Chaudhuri, Journal of hazardous materials, 173, 445 (2010).
- [7] L. Wang, Y. Zheng, X. Li, W. Dong, W. Tang, B. Chen, C. Li, X. Li, T. Zhang and W. Xu, Thin Solid Films, 519, 5673 (2011).
- [8] N. Padmavathy and R. Vijayaraghavan, Science and technology of advanced materials, 9, 035004 (2008).
- [9] D. Sharma, J. Rajput, B. Kaith, M. Kaur and S. Sharma, Thin solid films, 519, 1224 (2010).

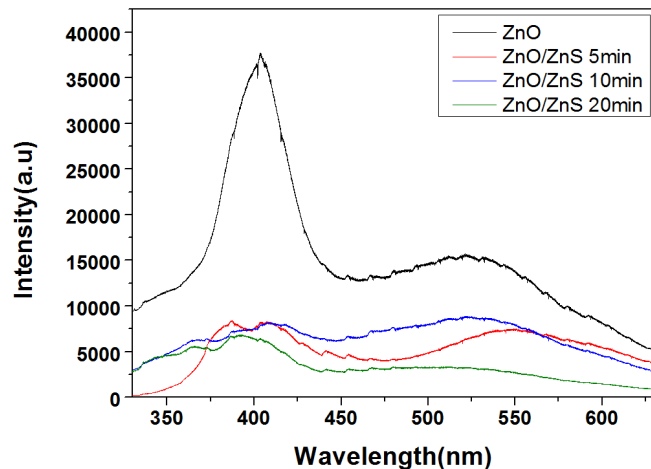


Figure 7. 300-650 nm PL measurement of the ZnO alone and ZnO/ZnS on the glass fiber at 5, 10 and 20 mins.

- [10] R. R. Gandhi, S. Gowri, J. Suresh and M. Sundrarajan, Journal of Materials Science & Technology, 29, 533 (2013).
- [11] A. Sirelkhatim, S. Mahmud, A. Seeni, N. H. M. Kaus, L. C. Ann, S. K. M. Bakhori, H. Hasan and D. Mohamad, Nano-Micro Letters, 7, 219 (2015).
- [12] T.-t. Wong, K.-t. Lau, W.-y. Tam, J. Leng and J. A. Etches, Materials & Design, 56, 254 (2014).
- [13] J. F. de Lima, R. F. Martins and O. A. Serra, Optical Materials, 35, 56 (2012).
- [14] T. T. X. Hang, N. T. Dung, T. A. Truc, N. T. Duong, B. Van Truoc, P. G. Vu, T. Hoang, D. T. M. Thanh and M.-G. Olivier, Progress in Organic Coatings, 79, 68 (2015).
- [15] L. Esteban-Tejeda, B. Cabal, R. Torrecillas, C. Prado, E. Fernandez-Garcia, R. López-Piriz, F. Quintero, J. Pou, J. Penide and J. S. Moya, Biomedical Materials, 11, 045014 (2016).
- [16] J. Cleveland and A. D. Weidemann, Limnology and Oceanography, 38, 1321 (1993).
- [17] R. John and S. Florence, Chalcogenide letters, 7, (2010).
- [18] H. R. Dizaji, A. J. Zavaraki and M. Ehsani, Chalcogenide Letters, 8, 231 (2011).
- [19] H. Ramli, S. K. A. Rahim, T. A. Rahman and M. M. Aminuddin, Chalcogenide Letters, 10, (2013).
- [20] T. Yu, K. Wang, Y. Chen, M. Sheu and H. Chen, Chalcogenide Letters, 14, (2017).